$^7Li(p,\pi^+)^8Li$ AND $^7Li(\vec{p},\pi^-)^8B$ REACTIONS AT T_p = 200 MeV

Z-J. Cao†, T.E. Ward§, R.D. Bent, J.D. Brown¶, E. Korkmaz, H. Nann, and T.G. Throwe††
Indiana University Cyclotron Facility, Bloomington, Indiana 47405

We have measured both differential cross sections and analyzing powers for the $^7Li(p,\pi^+)^8Li$ and $^7Li(p,\pi^-)^8B$ reactions, leading to the easily resolvable ground and first two excited states of ^8Li and ^8B, at bombarding energies of 200.4 and 199.2 MeV, respectively. These are the first measurements of the analyzing powers for these reactions.

By choosing light nuclei and a target for which the (p,π^+) and (p,π^-) reactions lead to isobaric analogue final states, it is hoped to minimize nuclear structure effects and uncertainties in the differences between the π^+ and π^- distorted waves, so that the dynamics of the (p,π^+) and (p,π^-) reactions will be more transparent.

The experiments were performed using polarized beams from the cyclotron having an energy spread of about 200 keV at a beam intensity ~200 nA. Pions were momentum analyzed using the QQSP spectrometer with the standard focal-plane detector array for pions.

The results are shown in Figs. 1 and 2. Our differential cross sections for the $^7Li(p,\pi^-)^8B$ reaction agree well with those of Kehayias.[1]

The nuclear structure and proton distortions are essentially the same for the two reactions, so the differences between the (p,π^+) and (p,π^-) data should reflect primarily the different dynamics of the elementary processes $pp \to d\pi^+$ and $pn \to pp\pi^-$, as well as different transition densities and Coulomb interactions. Thus, these data should help elucidate the microscopic mechanism of the pion production process in nuclei.

The $^7Li(p,\pi^-)^8B$ cross sections are generally of the order of 10 nb/sr - an order of magnitude smaller than those for the $^7Li(p,\pi^+)^8Li$ reaction. This may be explained qualitatively within the framework of the two-nucleon model by the different orbital angular momentum coupling of the intermediate Δ-isobar and nucleon. Explicitly, an intermediate S-wave isobar-nucleon system and p-wave pion emission dominate the $pp \to d\pi^+$ process, while a P-wave intermediate ΔN state and s-wave pion production dominate the $pn \to pp\pi^-$ reaction.[2] The S-wave ΔN amplitude is much larger than the P-wave amplitude near the pion production threshold. Besides the magnitudes of the cross sections, the shapes of the cross section angular distributions are quite different for the two reactions. Any successful microscopic model of pion production should be able to explain these differences in terms of the cross section angular distributions of the elementary subprocesses $pp \to d\pi^+$ and $pn \to pp\pi^-$ and the different transition densities.

The different dynamics of the underlining $pp \to d\pi^+$ and $pn \to pp\pi^-$ processes discussed above may lead to the different shapes of the analyzing power angular distributions for the $^7Li(p,\pi^+)^8Li$ and $^7Li(p,\pi^-)^8B$ reactions. The analyzing power angular distributions for the $^7Li(p,\pi^+)$ transitions to all three states of ^8Li shown in Fig. 1 have essentially the same shape as that of the $pp \to d\pi^+$ reaction near threshold (except for a kinematic shift of the minimum towards smaller angles). One notes that many different transition paths may contribute coherently to the (p,π^+) reaction, involving target nucleons from a variety of nuclear orbits. Averaging over these transition paths can result in a cancellation of any state-dependence of the analyzing power, so A_y then reflects essentially the

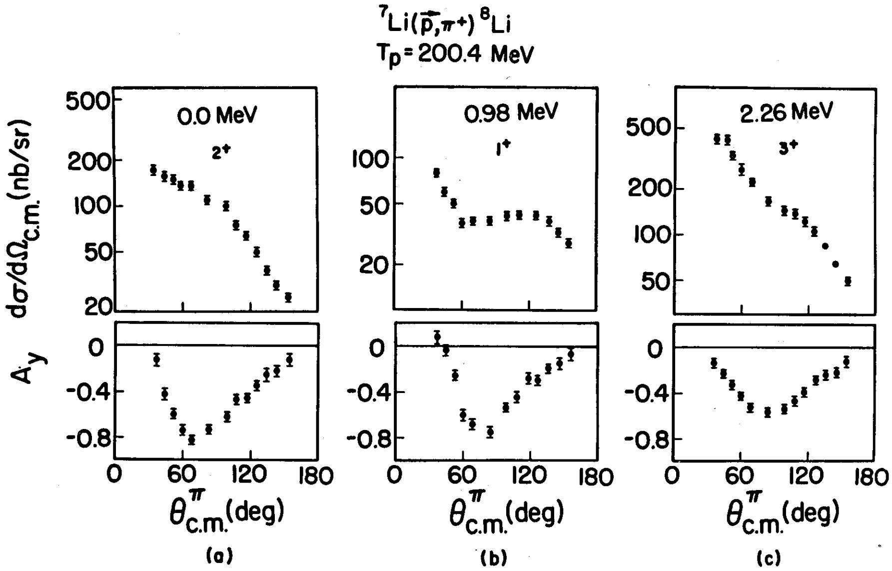

Figure 1. Angular distributions of the cross sections and analyzing powers for the $^{7}Li(p,\pi^{+})^{8}Li$ reaction leading to the ground, 0.98 MeV, and 2.26 MeV states of ^{8}Li at a bombarding energy of 200.4 MeV.

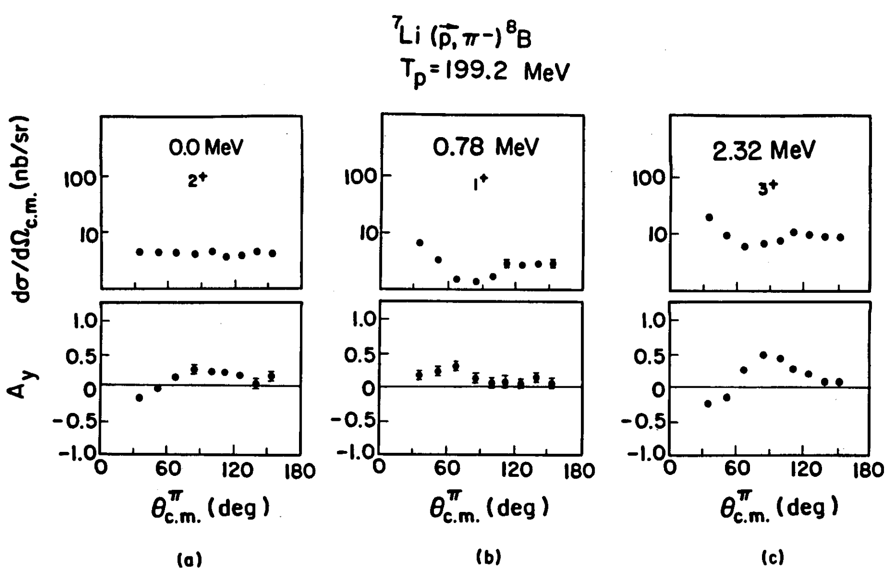

Figure 2. Angular distributions of the cross sections and analyzing powers for the $^{7}Li(p,\pi^{-})^{8}B$ reaction leading to the ground, 0.78 MeV, and 2.32 MeV states of ^{8}B at a bombarding energy of 199.2 MeV.

analyzing power of the underlying $pp \rightarrow \pi^{+}d$ process. Thus, our data provide further evidence for the dominance of the two-nucleon mechanism in the nuclear (p,π^{+}) process near threshold and exhibit features which may be characteristic of S-wave intermediate isobar-nucleon formation. In contrast, two types of analyzing power angular distributions are seen in the $^{7}Li(p,\pi^{-})^{8}B$ data. One of them is illustrated in Fig. 2(c). This pattern is quite similar to that observed for transitions to stretched two-particle one-hole states in near threshold (p,π^-) studies on a number of targets from A = 19 to A = 89.[1,3,4] This type of analyzing power angular distribution, which seems to be a "signature" of (p,π^-) transitions to stretched high-spin 2p-1h final states, is distinctly different from the other type illustrated by Fig. 2(b), which seems to be characteristic of transitions to low spin states. The state-dependence of the analyzing powers may result from a small analyzing power of the elementary $pn \rightarrow pp\pi^-$ process near the pion production threshold, which is suggested by recent studies[5] of the $^{13}C(p,\pi^-)^{14}O$ reaction leading to continuum final states, which essentially eliminate nuclear structure effects.

A qualitative explanation of the behavior of the analyzing power angular distributions described above for the $^7Li(p,\pi^-)^8B$ reaction, based on nuclear structure arguments, is the following. Shell model calculations performed using the computer code OXBASH[6] with the two-body interactions of Cohen and Kurath[7] and a model space restricted to the p-shell ($1p_{1/2}$ and $1p_{3/2}$ orbits) in the proton-neutron formalism give that the ^8B ground state, $J^\pi = 2^+$, is a mixture of 63% configuration (a), $[(\pi p_{3/2})^3_{J=3/2}\ (\nu p_{3/2})]$, and 14% configuration (b), $[(\pi p_{3/2})^2\ (\pi p_{1/2})\ (\nu p_{3/2})]$. In contrast, the 0.78 MeV, $J^\pi = 1^+$, state has 10% configuration (a) and 70% configuration (b). The 2.32 MeV, $J^\pi = 3^+$, state is an admixture of 63% configuration (a) and 24% configuration (c), $[(\pi p_{3/2})\ (\pi p_{1/2})^2_{J=0}\ (\nu p_{3/2})]$. Assuming a pure configuration $[(\pi p_{3/2})\ (\nu p_{3/2})^2_{J=0,2}]_{3/2^-}$ for the ^7Li ground state, a stretched two-particle one-hole configuration (with respect to the target nucleus) can couple to the initial target spin $3/2^-$ to give ^8B total spins and parities of $J^\pi = 2^+$ and 3^+ for configuration (a), $J^\pi = 2^+$, 3^+, and 4^+ for configuration (b), and $J^\pi = 0^+$, 1^+, 2^+, and 3^+ for configuration (c). Here, the term "stretched" refers to maximum spin for the two-particle one-hole angular momentum couplings, $[(\pi p_{3/2})^2_{J=2}\ (\nu p_{3/2})^{-1}]_{7/2}$, $[\{(\pi p_{3/2})(\pi p_{1/2})\}_{J=2}\ (\nu p_{3/2})^{-1}]_{7/2}$, and $[(\pi p_{1/2})^2_{J=0}\ (\nu p_{3/2})^{-1}]_{3/2}$, which lead to the final configurations (a), (b), and (c), respectively. The non-stretched 2p-1h configuration with two protons and one neutron hole in the $p_{3/2}$ orbit is $[(\pi p_{3/2})^2_{J=0}(\nu p_{3/2})^{-1}]_{3/2}$. Based on coefficients of fractional parentage, the stretched and non-stretched configurations contribute to case (a) with probabilities of about 83% and 17%, respectively. It follows from the above arguments that the ^8B ground state can be reached by an admixture of stretched and non-stretched two-particle one-hole configurations; the 0.78 MeV state involves non-stretched configurations only; and for the 2.32 MeV state, case (c) requires a pure stretched 2p-1h configuration and case (a) contains mainly the stretched component. These arguments are consistent with the stretched-state analyzing power signature for the 2.32 MeV state, a weaker stretched-state signature for the ground state, and no such signature for the 0.78 MeV state. With this interpretation, the data provide further evidence for the characteristic shapes of the analyzing power angular distributions for (p,π^-) transitions to 2p-1h stretched states, which are quite different from those for low spin transitions. This stretched-state signature has been used[8] as a spectroscopic tool to identify the spin structures of high-spin states preferentially populated in the (p,π^-) reaction.

It is hoped that the data presented here will provide useful tests of the microscopic model of nuclear pion production currently under development at IUCF.[9]

Present address:
†Physics Department, Carnegie-Mellon University, Pittsburgh, PA 15213.

§Department of Nuclear Energy, Brookhaven National Laboratory, Upton, NY 11973.

¶Physics Department, Princeton University, Princeton, NJ 08544.

††Physics Department, Physics Department, Brookhaven National Laboratory, Upton, NY 11973

1) J.J. Kehayias, Ph.D. Thesis, Indiana University, 1984 (unpublished).

2) T.S.H. Lee and K. Ohta, Phys. Rev. Lett. 49, 1079 (1982); R.R. Silbar and E. Piasetzky, Phys. Rev. C29, 1116 (1984).

3) T.G. Throwe, Ph.D. Thesis, Indiana University, 1985 (unpublished).

4) W.W. Jacobs, Proceedings of the Conference on Nuclear Structure at High Spin, Excitation, and Momentum Transfer, edited by H. Nann, AIP Conf. Proc. No. 142 (AIP, New York, 1986), p.181.

5) E. Korkmaz, Indiana University, private communication, 1986.

6) B.A. Brown, A. Etchegoyen, W.D.M. Rae, and N.S. Godwin, The Oxford-Buenos Aires Shell Model Code, 1984 (unpublished).

7) S. Cohen and D. Kurath, Nucl. Phys. A73, 1 (1965).

8) Z-J. Cao, R.D. Bent, H. Nann, and T.E. Ward, this Annual Report; and Phys. Rev. C35, (1987).

9) P.W.F. Alons et al., this Annual Report.

MEASUREMENT OF (p,π) AND (p,γ) REACTIONS BY RECOIL DETECTION*

J. Homolka, W. Schott, W. Wilhelm and W. Wagner
Physik-Department, Technische Universitat Munchen Garching, West Germany

R.D. Bent, M. Fatyga† and R.E. Pollock
Indiana University Cyclotron Facility Bloomington, Indiana 47405

R.E. Segel
Northwestern University, Evanston, Illinois 60204 and Argonne National Laboratory, Argonne, Illinois 60439

P. Kienle
Gesellschaft fur Schwerionenforschung Darmstadt, West Germany

K.E. Rehm
Argonne National Laboratory Argonne, Illinois 60439

M. Saber
Northwestern University, Evanston, Illinois 60204

Measurements of the $^{12}C(p,\pi^+)^{13}C$, $^{12}C(p,\pi^\circ)^{13}N_{g.s.}$ and $^{12}C(p,\gamma)^{13}N_{g.s.}$ reactions by recoil detection were continued at incident energies of 153.5, 166.1, 186.0 and 204.0 MeV. The recoils are detected in a focal-plane detector in the QQSP spectrometer.

The recoil products are analyzed by the magnetic spectrometer measuring $\frac{p}{Q}$, where p and Q are the recoil momentum and atomic charge, respectively. Combined with a measurement of time-of-flight through the spectrometer, the ratio $\frac{A}{Q}$ is determined, where A is the recoil atomic mass number. An energy loss measurement fixes the nuclear charge Z. The emission angle Θ is obtained by two position measurements using the heavy-ion detector. For reactions leading to a specific two-body final state the recoil products lie on a half-ellipse shaped contour in the p-Θ plane.[1]